Fe^{2+} in GaP studied by Fourier-transform emission and absorption spectroscopy

G. Rückert, K. Pressel, and A. Dörnen
4. Physikalisches Institut, Universität Stuttgart, D-7000 Stuttgart 80, Germany

K. Thonke
Abteilung Halbleiterphysik, Universität Ulm, D-7900 Ulm, Germany

W. Ulrici
Paul-Drude-Institut für Festkörperelektronik, D-1086 Berlin, Germany
(Received 21 January 1992)

We present an optical Fourier-transform-infrared photoluminescence (PL) and absorption study of the $^5T_2 \leftrightarrow {}^5E$ internal $3d$ transitions of Fe^{2+} in GaP. We analyze in detail the four zero-phonon lines of Fe^{2+} which appear at about 3300 cm^{-1} in GaP. A fine structure, which originates from different iron isotopes, is resolved. Detailed PL and absorption spectra between 2500 and 4200 cm^{-1} reveal many features in the Stokes and anti-Stokes phonon sidebands. With the help of temperature-dependent absorption measurements we are able to set up the complete level scheme for the internal $3d$ transitions of Fe^{2+} in GaP. We compare the experimental results to theoretical values obtained by crystal-field theory including spin-orbit coupling.

I. INTRODUCTION

$3d$ elements, such as Fe, are inadvertent and diffusive contaminations in III-V semiconductors and act as efficient recombination centers. The recombination channels introduced by these centers limit the efficiency of light emitting diodes which is determined by the near-band-gap emission.

Fe occurs in three different stable charge states in GaP. Both the existence of Fe^{3+} and the existence of Fe^{+} are shown by electron paramagnetic resonance.[1,2] The Fe^{2+} charge state is identified by optical measurements. A survey of spectroscopy on Fe doped InP, GaP, and GaAs has been published by Bishop.[3]

Fe is located on Ga sites in GaP. Both low-temperature photoluminescence (PL) and absorption spectra show a characteristic pattern of four Fe^{2+}-related zero-phonon (ZP) lines at about 3300 cm^{-1}. These lines are attributed to transitions within crystal-field states originating from the ^5D state of $Fe^{2+}(3d^6)$. The inset of Fig. 1(a) schematically shows the splitting of the ^5D ground state of the Fe^{2+} ion. Through the influence of the tetrahedral crystal field, caused by the four surrounding phosphorus atoms, the ^5D free-ion ground state is split into a lower state of character Γ_3 (or ^5E) and an upper state of character Γ_5 (or $^5T_2$). Additional spin-orbit (LS) coupling splits the $^5T_2$ excited state into a manifold of six sublevels (Γ_5, Γ_4, Γ_3, Γ_5', Γ_4', Γ_1). The ^5E ground state is split only via interaction with the $^5T_2$ excited state into five close lying, approximately equidistant sublevels (Γ_1, Γ_4, Γ_3, Γ_5, Γ_2 in ascending order).[4] In low-temperature PL measurements transitions between the lowest Γ_5 state of the $^5T_2$ manifold and the Γ_1, Γ_4, Γ_3, and Γ_5 levels of the ^5E manifold are observed routinely. These transitions are indicated by arrows labeled as 1–

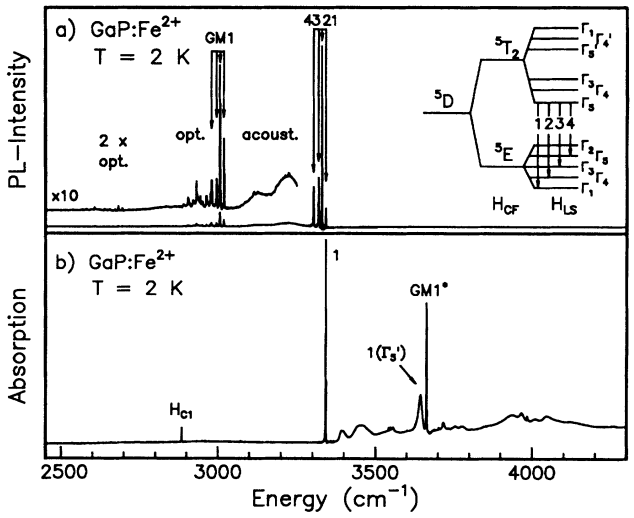

FIG. 1. (a) Inset: Level scheme of $Fe^{2+}(3d^6)$ in GaP. The ^5D free-ion ground state of Fe^{2+} is split by the tetrahedral crystal field and spin-orbit coupling interactions. The four electric dipole allowed transitions, observed in PL, are indicated by the four arrows labeled 1–4. The FTIR PL spectrum shows the four ZP lines at about 3340 cm^{-1}, which are labeled according to the inset. The Stokes phonon sideband shows coupling to acoustic and optic-type modes. Superimposed on the phonon sideband replicas due to several Fe-defect specific modes appear, e.g., GM1. (b) Absorption spectrum of Fe^{2+} in GaP. According to Boltzmann's law only ZP1 appears in the 2-K spectrum. The anti-Stokes absorption phonon sideband shows coupling to lattice modes and Fe-defect specific modes, which appear also in the PL Stokes-phonon sideband. Superimposed on the anti-Stokes phonon sideband also, transitions from the ^5E ground state to excited states of the $^5T_2$ manifold are observed [$1(\Gamma_5')$].

4 in the inset of Fig. 1(a). Symmetry rules do not allow optical transitions between the highest state of ^5E with character Γ_2 and the Γ_5 ground state of $^5T_2$.[5] The Fe^{2+}-related transitions were first observed in absorption measurements by Baranowski, Allen, and Pearson.[6] Later they were also detected in PL.[7,8] West *et al.*[9] have presented a detailed PL study of the four ZP lines, including Zeeman and uniaxial stress measurements. Up to now only Clark and Dean[8] have published a rough structure of the PL Stokes phonon sideband. Optical studies by conventional absorption spectroscopy[7,10] and calorimetric absorption spectroscopy[11] also have revealed only a rough structure of the anti-Stokes phonon sideband. From these absorption spectra it was not possible to distinguish between lines associated with phonon replicas and lines caused by electric dipole transitions between the ^5E ground state and the excited substates of the $^5T_2$ upper level.

In our Fourier-transform infrared (FTIR) PL and absorption measurements we observe numerous new features in the ZP lines and phonon sidebands. Additionally, we obtain information about the energetic position of the various sublevels of the ^5D state of Fe^{2+} in GaP.

In PL measurements we excited the samples with the 647-nm red line of a krypton-ion laser. In absorption measurements the light of a Globar has been used. Both PL and absorption spectra were recorded with a Bomem DA3.01 FTIR spectrometer (maximum unapodized resolution: 0.01 cm^{-1}), which has been equipped with a liquid-nitrogen-cooled InSb detector. Uncontrolled microscopic strain on the samples was avoided by careful mounting of the samples on the sample holder.

II. ZERO-PHONON LINES OF Fe^{2+} IN GaP

The FTIR PL spectrum in Fig. 1(a) shows the four characteristic ZP lines of Fe^{2+} around 3300 cm^{-1} (labeled 1–4) and the corresponding multiply structured Stokes phonon sidebands. The spectrum reveals many sharp lines which are superimposed on the phonon sideband. These lines will be discussed later in terms of coupling to Fe-defect specific phonons. According to Boltzmann's law the $\Gamma_1(^5E)$ state is the only state occupied at low temperature. Thus in absorption only ZP1 appears at 2 K [see Fig. 1(b)]. On the high-energy side the anti-Stokes phonon sideband shows up. Superimposed on this absorption phonon sideband additional peaks appear that have no counterpart in PL, e.g., the one labeled $1(\Gamma_5')$. As will be shown in Sec. IV, these peaks must be interpreted as transitions to higher states of the $^5T_2$ manifold. The peak at 2885.5 cm^{-1} in Fig. 1(b), labeled as H_{c1}, is not related to Fe^{2+}. Different from all other spectroscopic features, H_{c1} is still visible at room temperature with a half-width still small. This line recently has been identified as the stretching vibrational mode of the (N_p,H) complex.[12] In Table I the spectroscopic data of the energetic positions of the four ZP lines, their half-widths, and the relative spacings are summarized. As already found by West *et al.*[9] the spacings of the four ZP lines are not equidistant. Analogous to the systems Fe^{2+} in InP (Refs. 13 and 14) and Fe^{2+} in GaAs,[15] the splitting parameters of the ^5D ground state were determined. We solved numerically the following Hamiltonian which includes the crystal-field contribution H_{CF} and the spin-orbit coupling H_{LS}:

$$H = H_{CF} + H_{LS} = B_4(O_4^0 + 5O_4^4) + \lambda LS, \qquad B_4 = -Dq/12, \quad L = 2, \quad S = 2. \tag{1}$$

O_4^0 and O_4^4 are the Stevens's equivalent operators.[16] In this approximation the splitting is determined by the crystal-field parameter Dq and the spin-orbit coupling parameter λ. We fitted the theoretical values to the experimental transition energies of ZP1 to ZP4. Best accordance between theory and experiment was obtained with $Dq = 355.2$ cm^{-1} and $\lambda = -92.66$ cm^{-1}. These values are slightly different from those of West *et al.*,[9] who obtained $Dq = 355.9$ cm^{-1} and $\lambda = -93.5$ cm^{-1}. The reduction of the spin-orbit coupling parameter λ from its free-ion value $\lambda_0 = -103$ cm^{-1} is moderate. As shown in Table I our theoretical values of the spacings of the four ZP lines differ slightly from the experimental ones. As already pointed out by West *et al.*[9] and shown in more detail in a recent paper by Vogel *et al.*,[17] a dynamical Jahn-Teller effect can account for the difference between theoretical and experimental values for the spacing of the four ZP lines of Fe^{2+}. In addition, a more accurate theory has to take into account not only the Jahn-Teller effect, but also mixing with excited electronic Fe^{2+} states (e.g., $3d^54p$). The latter contribution is not negligible, since only mixing with these excited states of odd parity makes the internal $3d$ transitions of $Fe^{2+}(3d^6)$ electric dipole allowed. The covalent character of the bindings may also contribute to the wave functions.

As shown in Table I the four ZP lines have different values of the full widths at half maximum (FWHM) in PL at 2 K. While the two high-energy peaks (ZP1 and ZP2) have a FWHM of $\simeq 0.2$ cm^{-1} in our samples, the two low-energy peaks (ZP3 and ZP4) have a FWHM of more than 1 cm^{-1}. Analogous to the InP:Fe^{2+} case,[13] the lines ZP1 to ZP4 possess essentially Lorentzian line shape. We assume that the two broader lines ZP3 and ZP4 are lifetime broadened due to a fast phonon relaxation process from their final states $\Gamma_3(^5E)$ and $\Gamma_5(^5E)$ to the lower states $\Gamma_1(^5E)$ and $\Gamma_4(^5E)$. For the $\Gamma_4(^5E)$ state a nonradiative relaxation to the lowest $\Gamma_1(^5E)$ state is forbidden by selection rules. From this fact a significantly longer lifetime is expected for the $\Gamma_4(^5E)$ state. This is the reason that both ZP1 and ZP2 have the same small half-width of only $\simeq 0.2$ cm^{-1}. In absorption measurements at 2 K sample temperature we find for ZP1 also Lorentzian line shape and a FWHM of about 0.18 cm^{-1}. Thus in contrast to the value of the FWHM of ZP1 in InP:Fe,[13] where we excited the samples with above band-gap light of a Kr-ion laser, the FWHM of ZP1 in GaP:Fe is found to be about the same in absorption and PL in all our samples at 2.1 K. Recent PL measurements on InP:Fe using also below band-gap excitation light of a Ti/sapphire laser showed that the FWHM in PL and absorption becomes about the same, too. For higher sample temperatures

(T >5 K), both ZP1 and ZP2 exhibit purely Lorentzian shape. This hints to lifetime effects accounting for the line broadenings. Figure 2 shows the temperature dependence of the FWHM of ZP1 and ZP2 between 2 K and 28 K. In the inset the temperature range between 10 K and 21 K is shown in more detail. For temperatures below 4.2 K the half-width approaches a limit of 0.18 cm^{-1}. The corresponding lifetime is $\cong 0.3 \times 10^{-13}$ sec. This short lifetime must be determined by nonradiative processes, since the radiative lifetime is on the order of $\simeq 10$ μsec.[18] For temperatures above 6 K an obviously thermally activated process leads to broadening. The temperature dependence of the FWHM thus can be described by the empirical law

$$\Delta E_{\mathrm{FWHM}}(T) = F_0 + F_1 \exp(-E_1/k_bT) . \qquad (2)$$

The half-width of the lifetime broadened transition is $\hbar/\tau$, with $1/\tau = 1/\tau_i + 1/\tau_f$, where τ_i and τ_f are the effective lifetimes of the initial and final state, respectively. Both τ_i and τ_f might be shortened by thermally activated processes. From a numerical fit of Eq. (2) to the values of the change of the half-width of ZP1 and ZP2 with temperature we find for E_1 values of 43 $\pm$ 5 cm^{-1} for ZP1 and 39 $\pm$ 5 cm^{-1} for ZP2. The low-temperature limit F_0 of the halfwidth is 0.18 cm^{-1} for both lines, and the high-temperature limit F_1 is 35 $\pm$ 3 cm^{-1} for ZP1 and 23 $\pm$ 3 cm^{-1} for ZP2. The determined activation energy of $\simeq 40$ cm^{-1} could hint to thermal ejection of carriers from the $\Gamma_5(^5T_2)$ state to the next excited state (see Sec. IV and Fig. 7). The prefactor F_1 of $\simeq 30$ cm^{-1} then would mean that the transitions from the next higher states $\Gamma_3(^5T_2)$ or $\Gamma_4(^5T_2)$ must have lifetimes, which are approximately two orders of magnitude shorter than those starting on the lowest $\Gamma_5(^5T_2)$ state. Numerical evaluation of the transition matrix elements derived from eigenvectors of Hamiltonian (1) show that the total transition probability of $\{\Gamma_5(^5T_2) \rightarrow {}^5E\}$ and $\{\Gamma_4(^5T_2) \rightarrow {}^5E\}$ is about the same, and that of $\{\Gamma_3(^5T_2) \rightarrow {}^5E\}$ is even lower. Due to influences of a dynamical Jahn-Teller effect these matrix elements might be altered, but we do not expect too dramatic changes. Thus, again nonradiative processes with even higher probabilities must form a parallel channel, which is opened by thermal activation. An assignment to radiative transitions must be ruled out, since no trace of such a significntly more allowed excited transition $\simeq 40$ cm^{-1} above ZP1 is found in the absorption sprectrum (see the next section).

An alternative explanation for the thermally activated

TABLE I. Spectral data of the zero-phonon lines of Fe^{2+} in GaP. The values are extracted from spectra recorded at 2 K sample temperature, except the energies of the "hot lines," which refer to $\simeq$ 20 K sample temperature.

Line	Energy absolute / relative (cm^{-1})				FWHM (cm^{-1})	
	Absorption	PL	Spacing	Theory	PL	Absorption
1 (^{54}Fe)	3341.9	3341.9				
1 (^{56}Fe)	3342.3_5	3342.3_5		3342.4	0.18	0.18
1 (^{57}Fe)		3342.6				
1 (^{58}Fe)		3342.8	12.9			
2 (^{54}Fe)		3329.0_5				
2 (^{56}Fe)	3329.5	3329.5		3330.1	0.18	
2 (^{57}Fe)		3329.7				
2 (^{58}Fe)		3330.0	10.8			
3	3318.7	3318.7		3317.6	1	
4	3302.5	3302.7	16.2	3303.0	1.3	
$2(\Gamma_3)$	3378			3535.5		
$2(\Gamma_4)$	3416			3519.4		
			11			
$3(\Gamma_4)$	3405			3508.6		
$4(\Gamma_4)$	3389					
$1(\Gamma_5')$	3644.8			3801.9	4.7	
			12.8			
$2(\Gamma_5')$	3632			3789.5		
$3(\Gamma_5')$	3621					
$4(\Gamma_5')$	3605					
$2(\Gamma_4')$	3694.3					
$3(\Gamma_4')$	3705.2					

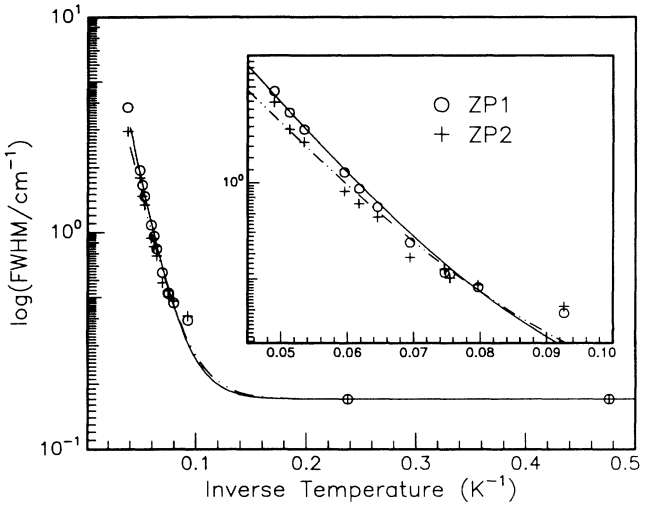

FIG. 2. Temperature dependence of the absorption halfwidth of ZP lines 1 and 2 between 2 and 28 K. As the line shape is Lorentzian, the full width at half maximum (FWHM) is determined by lifetime effects. In both curves the lifetime is reduced by thermally activated processes with $\simeq 40$ cm^{-1} activation energy (see text).

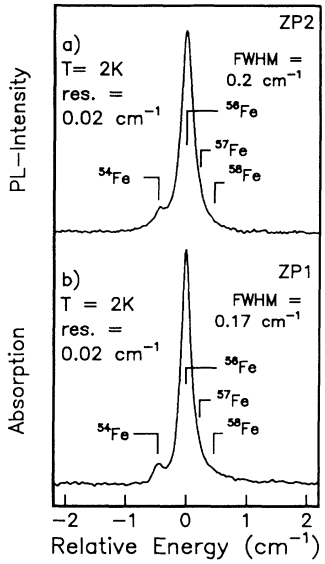

FIG. 3. (a) High-resolution PL spectrum of ZP2, the most intense Fe^{2+} line in luminescence. Analogous to the case of Fe^{2+} in InP (see Ref. 13) the twofold fine structure is introduced by ^{54}Fe and ^{56}Fe isotopes. The weak high-energy tail originates from ^{57}Fe and ^{58}Fe contributions. (b) Fine structure in the absorption spectrum of ZP1, which is the most intense ZP line at 2 K. ZP1 shows the same fine-structure splitting as ZP2 in PL. Again, the high-energy tail due to contributions of ^{57}Fe and ^{58}Fe appears.

broadening might be sought in the thermal release of shallow bound holes or electrons, which can shorten the lifetime of the Fe^{2+} centers due to charge transfer processes by capture of these released particles. Such a notion would fit better to the high-temperature limit F_1, but the activation energy is clearly distinct from the binding energies for shallow common donors and acceptors in GaP, which are in the range of 400–1000 cm^{-1}. From their PL lifetime measurements Klein and Weiser[18] deduce a capture time for holes of $\simeq 10$ μsec, which is much slower than the rates required to account for the halfwidth of $\simeq 30$ cm^{-1}.

Another possibility is the thermally activated transfer of excitation from Fe^{2+} to some other defect, but we do not have clear indications for such a transfer. Thus, the origin of the thermal broadening of the Fe^{2+} transitions remains unclear at present.

Optical FTIR spectroscopy reveals a new fine structure in the Fe^{2+}-related ZP lines. Figure 3(a) shows a high-resolution PL spectrum of transition ZP2, which is the most intense line in PL at low sample temperatures. The spectrum clearly shows a fine structure splitting of ZP2 into two peaks, which are separated by 0.46 cm^{-1}. In the case of InP:Fe Pressel *et al.*[13] observed an equivalent fine structure in the Fe^{2+} ZP lines and demonstrated unambiguously by experiments on ^{54}Fe implanted samples that the splitting is due to an isotopic effect. In absorption measurements on GaP:Fe^{2+} only ZP1 shows up at 2 K. As depicted in Fig. 1(b) ZP1 exhibits the identical isotopic splitting. The intensity ratio ascribed to the ^{54}Fe and ^{56}Fe components excellently fits to the natural abundance of the four stable iron isotopes [^{54}Fe (5.8%),^{56}Fe (91.8%),^{57}Fe (2.1%), and ^{58}Fe (0.3%)]. In InP the line shapes of the four ZP lines are narrower than in GaP and therefore Pressel *et al.*[13] were able to observe the weaker peaks due to the rarer isotopes Fe^{57} and Fe^{58}, too. The extended high-energy tail of the GaP:Fe ZP1 and ZP2 lines hints to contributions of the ^{57}Fe and ^{58}Fe isotopes.

III. PHONON SIDEBANDS

A. Phonon sidebands in photoluminescence

Figure 4 shows detailed low-temperature PL spectra of the Stokes phonon sideband, which can be subdivided into three regions: the region of coupling to acoustical-type phonons between 3050 and 3300 cm^{-1} [see Fig. 4(a)], the region of coupling to optical-type phonons between 2850 and 3050 cm^{-1} [see Fig. 4(b)], and the region of two-phonon coupling between 2530 and 2730 cm^{-1} [see Fig. 4(c)]. Generally, we assign the broad humps to coupling of the Fe^{2+}-related ZP transitions to undisturbed lattice phonons, and we attribute the sharp lines to coupling to Fe^{2+} defect specific phonons. The coupling of the four ZP transitions to several Fe^{2+} defect specific modes leads to a characteristic series of sharp lines with spacings identical to the spacings of the four ZP lines. These series of vibrational replica are indicated by sets of arrows in Figs. 4(a)–4(c).

In Fig. 4(a) the broad feature peaking at 3220 cm^{-1} corresponds to coupling to TA phonons. The energetic distance to the ZP lines fits to a superposition of

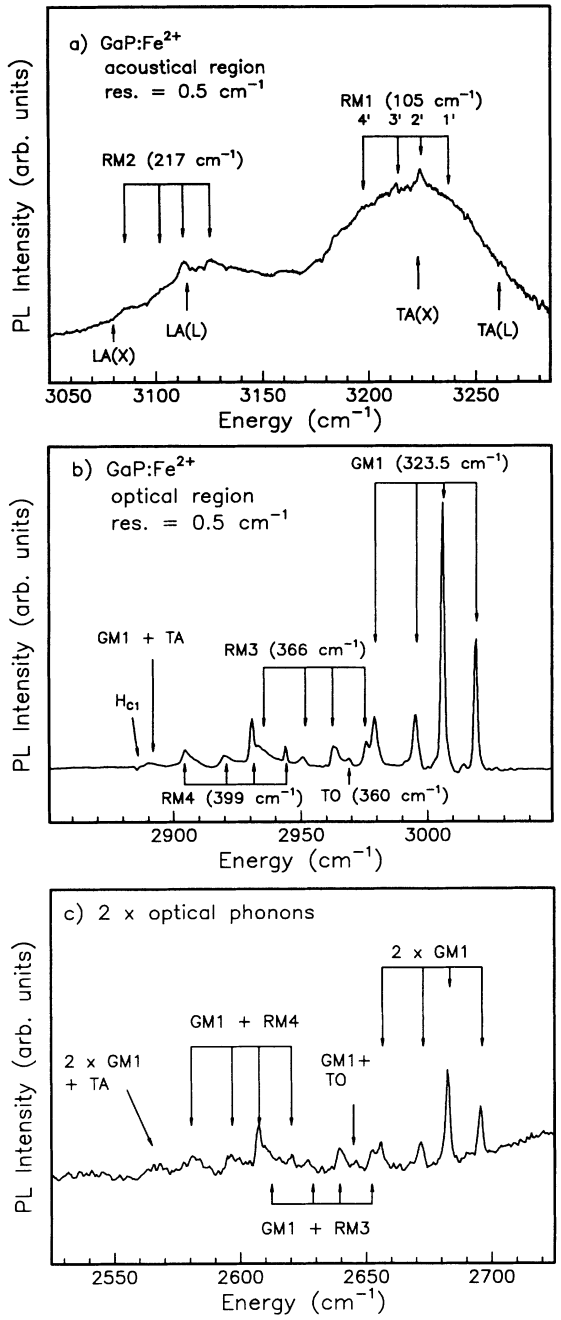

FIG. 4. (a) Phonon sideband in the acoustical region. In addition to coupling of the four ZP transitions to undisturbed TA and LA lattice modes (the positions of the TA and LA modes according to Ref. 19 are indicated by arrows) we observe two sharper series of replicas labeled RM1 and RM2. Note that for RM1 the phonon coupling to ZP1 is missing. This observation is analogous to the RM1 mode in the InP:Fe^{2+} case (see Ref. 13). (b) Phonon replicas in the optical region. We observe three series of lines which are introduced either by coupling to a gap mode (GM1) or coupling to resonant modes (RM3 and RM4). Weaker peaks in between are interpreted as replicas due to lattice modes or combinations of these. (c) The spectrum shows the region of coupling to two optical phonons. The spectrum is similar to the one-optical-phonon region depicted in (b), but shifted by another GM1 phonon energy of 323.5 cm^{-1}.

the TA(X) and TA(L) phonons, which have energies of 68 and 106 cm^{-1}, respectively.[19] The broad resonance with maximum at about 3120 cm^{-1} is attributed to coupling to LA(L) and LA(X) crystal phonons, which have phonon energies of 215 cm^{-1} [LA(L)] and 250 cm^{-1} [LA(X)], respectively.[19] Superimposed on these two humps we observe two weakly coupling Fe^{2+} defect specific resonant modes (RM) with energies of 105 cm^{-1} (RM1) and 217 cm^{-1} (RM2), respectively. Analogous to the InP:Fe case,[13] the resonant mode with lowest energy (105 cm^{-1} for GaP:Fe^{2+}, 100 cm^{-1} for InP:Fe^{2+}) does not couple to the transition ZP1. The assignment of the phonon replicas is unique, since the spacing of lines 2' and 3' in Fig. 4(a) coincides with the spacing of ZP2 and ZP3.

In the region of coupling to optical-type phonons [Fig. (4b)] we observe replicas of two resonant modes with energies of 366 cm^{-1} (RM3) and 399 cm^{-1} (RM4). The most prominent feature in this spectral region is introduced by coupling to a defect-induced gap mode (GM1). The low half-widths of these replicas (< 0.8 cm^{-1}) confirm this assignment. From the energetic distance of the four lines ZP1 to ZP4 to the GM1 replica a vibrational energy of 323.5 cm^{-1} results. The weak peak at 2969 cm^{-1}, which has an energetic distance of 360 cm^{-1} to ZP2, is attributed to coupling to a TO phonon. The broad signature at 2890 cm^{-1} is assigned to coupling to a combination of GM1 + TA. The peak H_{c1}, showing up in absorption at 2885.5 cm^{-1} [see Fig. 1(b)], appears also as a small dip in the emission phonon sideband at the same position. The overall shape of the phonon sideband in the optical phonon region (if mode RM3 is neglected) is very similar to that of InP:Fe^{2+},[13] where the Fe^{2+} ion is embedded also in a shell of four phosphorus atoms as first neighbors. Two-phonon replicas, introduced by coupling of the ZP transitions to 2 × GM1 and combinations

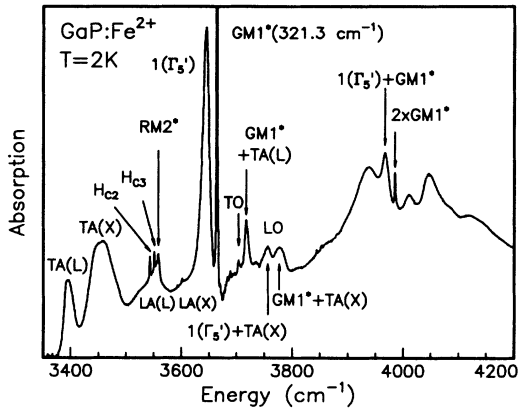

FIG. 5. Absorption phonon sideband of the Fe^{2+} transitions in GaP. Most vibrational modes that couple in emission are also observed in absorption. The gap mode GM1* is found in the phonon-related part of the absorption sideband as the strongest feature, too. Additional peaks are found that have no counterpart in the PL phonon sideband. They are attributed to internal electronic transitions from the ^5E manifold to excited $^5T_2$ states.

of GM1 with RM3, RM4, etc., are found in the energy region around 2600 cm^{-1} [see Fig. 4(c)]. This spectrum essentially looks like the one-optical-phonon region shifted by another GM1 phonon energy.

B. Phonon sidebands in absorption

As shown in Fig. 1(b), at low sample temperatures (T = 2 K) ZP1 dominates the absorption spectrum, since mainly the lowest initial level $\Gamma_1(^5E)$ is populated. Thus only the phonon replicas of ZP1 are found in the phonon sideband. Figure 5 shows the anti-Stokes phonon sideband in more detail. Similar to the cases InP:Fe (Ref. 14) and GaAs:Fe,[15] the coupling to the Fe^{2+} defect specific resonant modes is weaker in absorption than in PL. Only the coupling to the gap mode GM1 is as clearly visible as in PL, whereas the replicas due to the resonant modes are rather weak or even not detectable on the broad background. The energy of this Fe^{2+} specific gap mode GM1* is 321.3 cm^{-1}, i.e., the energy of this vibration is slightly different when Fe^{2+} is either in its excited $^5T_2$ state or in its ^5E ground state [$\hbar\Omega$ (GM1) = 323.5 cm^{-1}]. In Fig. 5 the peak corresponding to GM1* is cut to reveal also the less intense features. For both RM2* (anti-Stokes counterpart of mode RM2) and GM1* the replicas of the ZP2 to ZP4 lines, which emanate from excited substates of the ^5E manifold, show up with rising sample temperature (see Fig. 6).

Closest to ZP1 the double-peaked counterpart of the TA(L) and TA(X) emission phonon replica is found. Superimposed on the hump at 3550 cm^{-1}, which is attributed to the anti-Stokes counterpart of the LA(L) replica, we observe three sharp lines. These peaks are shown in an enlarged scale in Fig. 6. As obvious from the temperature-dependent measurements only the line at 3558 cm^{-1} and the hot line at 3545 cm^{-1} thermalize like the ZP lines. We identify these lines with the anti-

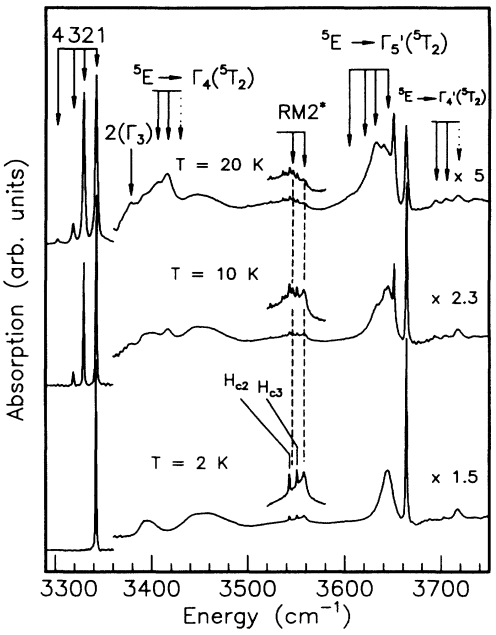

FIG. 6. Absorption spectra of the 3d internal transitions of Fe^{2+} recorded at different sample temperatures. Besides the four ZP lines 1–4 we observe several electronic transitions from the ^5E ground state manifold to excited $^5T_2$ states (see Fig. 7). Sets of arrows point to transitions starting on different ^5E states, but ending in a common $^5T_2$ substate. Arrows consisting of dots indicate forbidden transitions.

TABLE II. Spectral data for phonon replicas of the Fe^{2+} internal 3d transitions in GaP in PL [Figs. 4(a)–4(c)] and absorption (Fig. 5). The energies of the defect specific modes GM1 and RM2 are slightly different when the defect is in the final ^5E state (PL) or in the final $^5T_2$ state (absorption; modes denoted by an asterisk). ‡ indicates the center of a broad peak.

Photoluminescence		Absorption	
Relative energy (cm^{-1})	Interpretation	Relative energy (cm^{-1})	Interpretation
~ 68‡	TA(L)	~ 54‡	TA(L)
~ 106‡	TA(X)	~ 113‡	TA(X)
105	RM1		
~ 215‡	LA(L)	215	LA
~ 250‡	LA(X)		
217	RM2	216	RM2*
323.5	GM1	321.3	GM1*
360	TO	360	TO(L, X)
		375	GM1* + TA(L)
366	RM3		
399	RM4		
2 × 323.5	2 × GM1	2 × 321.3	GM1*
323.5 ± 360	GM1 ± TO(L, X)		
323.5 ± 366	GM1 ± RM3		
323.5 ± 399	GM1 ± RM4		

Stokes replicas RM2* of the ZP lines. The energetic distance of this peak to ZP1 is 216 cm^{-1} and thus is slightly altered from the RM2 mode ($\hbar\Omega = 217$ cm^{-1}) generated in the Fe^{2+} ^5E state, the mode which is observed in PL. The present data indicate that the other narrow lines at 3543 cm^{-1}(H_{C2}) and 3551 cm^{-1}(H_{C3}) cannot be related to Fe^{2+}. We observe no counterpart in the Stokes PL phonon sideband. Also the spacing between H_{C2} and H_{C3} does not agree with any of the spacings of the four ZP lines of Fe^{2+}. As the two peaks remain relatively sharp and observable even at sample temperatures above 50 K, we tentatively ascribe these lines to vibrational excitations of hydrogen related complexes. Therefore the attribution to a Fe^{2+} related resonant mode suggested recently[11] must be ruled out.

We attribute the weaker peaks between 3700 and 3800 cm^{-1} to couplings to optical-type phonons. Especially the peak at 3705 cm^{-1} is ascribed to a TO phonon replica ($\nu_{TO} = 360$ cm^{-1}), and the peak at 3717 cm^{-1} to a GM1* + TA(L) phonon replica. At even higher energies we observe a two-phonon replica 2 × GM1* of ZP1, and coupling of GM1* to the internal Fe^{2+} transition 1(Γ_5'). The spectral data of the phonon replica are summarized in Table II.

Superimposed on the absorption phonon sideband we observe peaks that have no counterpart in the PL phonon sideband, e.g., the peak labeled 1(Γ_5') (Fig. 5). These peaks, which we ascribe to transitions to higher substates of $^5T_2$, will be discussed in the following section.

IV. THE LEVEL SCHEME OF Fe^{2+} IN GaP

With increasing sample temperature, some "hot line" transitions starting on higher ^5E substates add to the spectrum. Careful analysis of spectra recorded at different sample temperatures and comparison with the PL phonon sideband help us to distinguish between phonon related and electronic features. Line positions, selection rules, and the thermalization properties of the observed lines (see Fig. 6) allow us to establish the level scheme depicted in Fig. 7.

The absorption spectra of Figs. 1(b) and 5, both recorded at 2 K, reveal a peak at 3644.8 cm^{-1}, which we labeled 1(Γ_5'). This peak has no counterpart in PL. At 2 K sample temperature only the Γ_1 state of the ^5E manifold is occupied. Selection rules allow electric dipole transitions only from a state of symmetry Γ_1 to states of symmetry Γ_5. Hence we assign the peak at 3644.8 cm^{-1} (i.e., 302.5 cm^{-1} above ZP1) to the transition from the $\Gamma_1(^5E)$ ground state into the Γ_5' ($^5T_2$) excited state. The FWHM of the ZP line 1(Γ_5') is approximately 5 cm^{-1}, which is about 30 times larger than the FWHM of ZP1. Since electrons in the excited $\Gamma_5'(^5T_2)$ state can relax fast into the $\Gamma_5(^5T_2)$ ground state of the $^5T_2$ manifold via nonradiative processes, an increased half-width due to lifetime broadening is expected. The corresponding transitions with similar energetic distance to the four "normal" ZP lines of Fe^{2+} and with similar half-widths also have been found for the systems InP:Fe (Ref. 14) and GaAs:Fe.[15]

From the first excited ^5E state with character Γ_4 electric dipole transitions to $\Gamma_5, \Gamma_4, \Gamma_3$, and Γ_2 states are allowed. From the middle ^5E state (character Γ_3), electric dipole transitions to states of character Γ_4 and Γ_5 are allowed, but not to Γ_3.

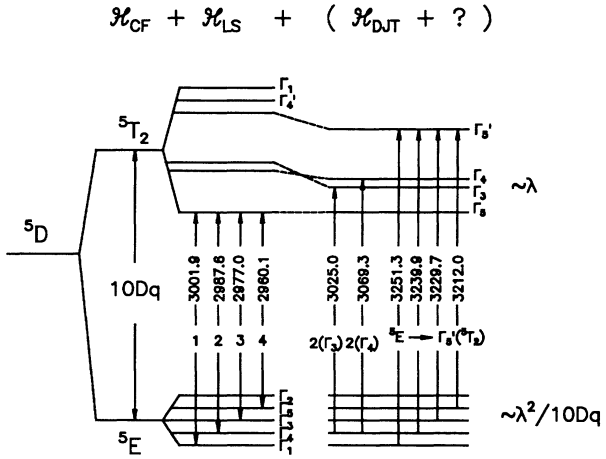

FIG. 7. Level scheme of Fe^{2+} in GaP. The ^5D free-ion ground state of Fe^{2+} is split by crystal-field and spin-orbit interactions. The positions of the $^5T_2$ substates depend linearly on the spin-orbit coupling parameter λ. The positions of the ^5E substates are proportional to λ^2/Dq (Ref. 4). The arrows indicate the optical transitions observed in PL and absorption. The numbers included in the arrows give the observed experimental transition energies in cm^{-1}. The parameters Dq and λ were fit to the experimental values of the four ZP lines 1–4. Compared to the energetic positions obtained by the fit the experimental values of the $^5T_2$ excited states are lower. These lowerings are shown to the right of the $^5T_2$ states. The shift to lower energies can be explained by a dynamical Jahn-Teller effect. Additionally, as indicated by the question mark the lowering might also be due to covalency effects or mixing with higher energy states other than ^5D.

When the sample temperature is increased, also higher states of the ^5E manifold become populated thermally. All the allowed transitions show up in the absorption spectra and can be identified by coincidences of energetic spacings (see Fig. 6). In the spectra recorded at 10 and 20 K sample temperature the whole group of the ZP1 to ZP4 lines shows up with identical spacings, but shifted by 302.5 cm^{-1} to higher energy. These lines are indicated by the set of arrows labeled $^5E \rightarrow \Gamma_5'(^5T_2)$ in Fig. 6 and in the level scheme in Fig. 7. Approximately 72 cm^{-1} higher in energy, another series of lines comes up with increasing sample temperature. It consists of a line located at 3717.4 cm^{-1}, which is seen already at 2 K sample temperature, and two hot lines at 3705.2 and 3694.3 cm^{-1}. The spacing between the two hot lines is 10.8 cm^{-1} and thus (within experimental error) equals the spacing of the second and third ^5E levels. But the distance of the first mentioned "cold line" at 3717.4 cm^{-1} from its next neighbor (at 3705.2 cm^{-1}) is 12.3 cm^{-1} and thus clearly different from the two lowest ^5E states. There exist two possible explanations for these lines: (i) These are transitions from the ^5E ground state to another excited state of character Γ_5 – a state which can be an excited vibronic state in a Jahn-Teller series.[17] (ii) The cold line

(at 3717.4 cm^{-1}) is a phonon combination replica (GM1* + TA) of line ZP1, and the two hot lines just below must be ascribed to the allowed transitions $\Gamma_4(^5E) \rightarrow \Gamma_4'(^5T_2)$ and $\Gamma_3(^5E) \rightarrow \Gamma_4'(^5T_2)$, respectively. Presently, we prefer the more straightforward second interpretation and used this assignment for the level scheme in Fig. 7.

Superimposed on the TA replica of the ZP1 to ZP4 lines, some other hot lines add in the spectra recorded at higher sample temperature (see Fig. 6). From their spacing of 11 cm^{-1}, the two lines at 3405 and 3416 cm^{-1} must be ascribed to transitions starting on the second and third lowest ^5E states. The transition beginning on the lowest ^5E state is obviously forbidden. From selection rules it follows that these transitions must end in a state with character Γ_4, i.e., these are the $^5E \rightarrow \Gamma_4(^5T_2)$ transitions.

Another hot line with an energy of 3378.2 cm^{-1} is ascribed to the transition $\Gamma_4(^5E) \rightarrow \Gamma_3(^5T_2)$, labeled $2(\Gamma_3)$ in Fig. 6. Thus, an inversion of the Γ_3 and Γ_4 states of ^5T must be inferred (Fig. 7), as was deduced already for the case of InP:Fe^{2+} (see Ref. 15).

Our theoretical approach, which includes crystal-field theory and spin-orbit coupling, predicts the Γ_5' to be 459 cm^{-1} higher in energy than the Γ_5 state. Also, the $\Gamma_3(^5T_2)$ is located 205 cm^{-1} above the $\Gamma_5(^5T_2)$ state and the $\Gamma_4(^5T_2)$ is located 189 cm^{-1} above the $\Gamma_5(^5T_2)$ state. Compared to the experimental values above, the theoretical calculation predicts the energy levels of the $^5T_2$ manifold too high. The size of the energetic shift of the experimental data to lower energy is indicated in the right-hand part of the level scheme in Fig. 7. All excited $^5T_2$ levels are lowered in energy by more than 100 cm^{-1}. Ham and Slack showed that the spacings can be significantly reduced by the influence of a dynamical Jahn-Teller (DJT) effect (see Fig. 5 in Ref. 20). For coupling of these states to Γ_3-type phonons with $\hbar\Omega < \lambda$, the $\Gamma_3(^5T_2)$ state can be pulled below the $\Gamma_4(^5T_2)$ state, the ordering we observe in our measurements.

V. SUMMARY

We present highly resolved PL and absorption spectra with improved signal-to-noise ratio for the electronic transitions of $Fe^{2+}(^5D)$ in GaP. A fine-structure splitting in the zero-phonon lines of the internal electronic transitions observed both in PL and in absorption is identified to be due to the four natural Fe isotopes. The PL Stokes phonon sideband reveals new couplings to different Fe-related vibrational modes. Comparison with the anti-Stokes phonon sideband observed in absorption enables us to identify several different lattice and Fe-related vibrational modes. The comparison of PL spectra with absorption measurements allows us also to distinguish between vibronic sidebands and ZP lines which emanate from the ^5E ground state manifold and end in the series of $^5T_2$ excited states. With the help of temperature-dependent absorption spectra we are able to derive the level scheme for the $^5E \rightarrow ^5T_2$ transitions. The experimentally determined splittings of the $^5T_2$ excited states are smaller than those theoretically predicted by a model calculation taking into account crystal-field and spin-orbit interaction. This discrepancy can be attributed to dynamical Jahn-Teller distortions.

[1] W. Ludwig and H. H. Woodbury, in *Solid State Physics, Advances in Research and Applications*, edited by F. Seitz and D. Turnbull (Academic, New York, 1962), Vol. 13, p. 208.

[2] U. Kaufmann and J. Schneider, Solid State Commun. **21**, 1073 (1977).

[3] S. G. Bishop, in *Deep Centers in Semiconductors*, edited by S. Pantelides (Gordon & Breach, New York, 1985), p. 541.

[4] W. Low and M. Weger, Phys Rev. **118**, 1119 (1960).

[5] G. F. Koster, J. O. Dimmock, R. G. Wheeler, and H. Statz, *Properties of the 32 Point Groups* (MIT, Cambridge, 1963).

[6] M. Baranowski, J. W. Allen, and G. L. Pearson, Phys. Rev. **160**, 627 (1967).

[7] A. V. Vasil'ev, G. K. Ippolitova, E. M. Omel'yanovskii, and A. I. Ryskin, Fiz. Tekh. Poluprovodn. **10**, 1201 (1976) [Sov. Phys. Semicond. **10**, 713 (1976)].

[8] G. Clark and P. J. Dean, in *Proceedings of the 14th International Conference on the Physics of Semiconductors*, edited by B. L. H. Wilson (Institute of Physics, London, 1979), Vol. 10, p. 1283.

[9] C. L. West, W. Hayes, J. F. Ryan, and P. J. Dean, J. Phys. C **13**, 5631 (1980).

[10] D. G. Andrianov, P. M. Grinshtein, G. K. Ippolitova, E. M. Omel'yanovskii, N. I. Suchkova, and V. I. Fistul', Fiz. Tekh. Poluprovodn. **10**, 1173 (1976) [Sov. Phys. Semicond. **10**, 696 (1976)].

[11] T. Wolf, D. Bimberg, and W. Ulrici, Phys. Rev. B **43**, 10 004 (1991).

[12] B. Clerjaud, D. Cote, W. S. Hahn, C. Porte, D. Wasik, and W. Ulrici, Appl. Phys. Lett. **58**, 1860 (1991).

[13] K. Pressel, K. Thonke, A. Dörnen, and G. Pensl, Phys. Rev. B **43**, 2239 (1991).

[14] K. Thonke and K. Pressel, Phys. Rev. B **44**, 13 418 (1991).

[15] K. Pressel, G. Rückert, K. Thonke, and A. Dörnen, Phys. Rev. B **46**, 13 171 (1992).

[16] A. Abragam and B. Bleaney, *Electron Paramagnetic Resonance of Transition Ions* (Clarendon, Oxford, 1970), pp. 372ff.

[17] E. E. Vogel, O. Mualin, M. A. de Orue, and J. Rivera-Iratchet, Phys. Rev. B **44**, 1579 (1991).

[18] P. B. Klein and K. Weiser, Solid State Commun. **41**, 365 (1982).

[19] *Numerical Data and Functional Relationships in Science and Technology*, Landolt-Börnstein, New Series, Vol. 17, Pt. a (Springer-Verlag, Berlin, 1982), pp. 281ff.

[20] F. S. Ham and G. A. Slack, Phys. Rev. B **4**, 777 (1971).